52

EXPERIENCE WITH THE X-15 AIRPLANE IN RELATION TO PROBLEMS OF REENTRY VEHICLES

ELDON E. KORDES
NASA Flight Research Center, Edwards, Calif.

ABSTRACT

This paper discusses some of the results obtained from the flight program of the X-15 research airplane that have application to the design philosophy of future glide reentry vehicles. Experiences in the areas of panel flutter, landing dynamics, flight control systems, and aerodynamic and structural heating are described, and some of the problems that have developed are discussed briefly. A bibliography of papers published on the X-15 flight program is included.

INTRODUCTION

The objectives of the X-15 program are to provide operational experience and research data on manned vehicles at hypersonic speeds and under reentry conditions. In order to accomplish these objectives within the state of the art, the X-15 airplane was designed on the basis of four flight trajectories: two for a maximum velocity of 6,600 fps and two for recovery from an altitude of 250,000 ft.

The X-15 was first flown in June 1959. Since then, 48 flights have been accomplished by a series of progressive steps to higher speeds and higher altitudes. Some deviations from this approach were made in order to investigate higher structural heating rates and aircraft stability at high angles of attack.

The X-15 program has provided much information in several areas of interest to designers of future hypersonic and reentry vehicles. The purpose of this paper is to present, briefly, some of the results of the program in the areas of panel flutter, landing dynamics, aerodynamic and structural heating, structural problems, handling qualities, and flight control systems. More complete information in these areas of the X-15 program and in other areas may be obtained from the papers listed in the bibliography.

AIRPLANE DESCRIPTION

The airplane that was built to meet the requirements of the four design flight trajectories mentioned previously is illustrated in Fig. 1, a cutaway drawing showing the internal arrangement of the aircraft.

The entire X-15 airplane is designed as a hot structure and is basically monocoque or semimonocoque construction. The external surface is Inconel X, and titanium is used extensively for the internal structure. The forward fuselage section contains double-wall pressure compartments for the pilot and instruments. The center fuselage section is formed by the oxidizer tank ahead of the wing and the fuel tank with frames for supporting the wing. The aft fuselage structure supports the empennage, the landing gear, and the engine. The wing is of multispar construction with Inconel X skin riveted to titanium substructure, and the horizontal and vertical tails are two-spar box structures with stabilizing ribs. The wing, horizontal tail, and vertical tail have segmented leading-edge heat sinks of Inconel X. A tunnel along each side of the fuselage for housing the control cables, hydraulic lines, and instrument wiring is formed by removable panels. Throughout the structure, extensive use has been made of corrugations and beading to minimize thermal stresses.

The landing gear consists of a full-castering nosewheel forward of the cockpit and two steel skids aft under the horizontal tail. All the aerodynamic control surfaces are contained in the empennage. The all-movable horizontal tail provides both roll and pitch control. Yaw control is provided by the all-movable rudder surfaces which form the top and bottom of the vertical tail. The lower rudder is jettisoned before each landing and recovered by parachute. Control at low dynamic pressure is provided by reaction-control rockets in the nose and in the wings. Stability augmentation is provided by a damper system in each control mode.

DISCUSSION OF RESULTS

PANEL FLUTTER

Panel flutter presented a problem on the first supersonic flights of the X-15 in the form of severe vibrations at high frequencies. The problem was solved without undue delay in the program by stiffening the affected panels. This

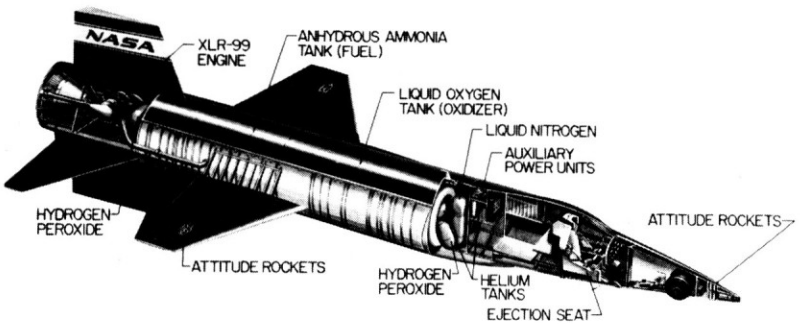

Fig. 1. X-15 Airplane.

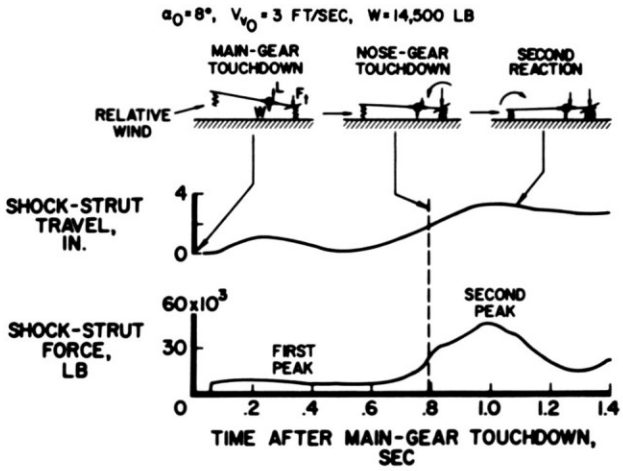

Fig. 2. Main-gear shock-strut force and travel.

experience showed clearly that very little was known about panel flutter and that more research effort was required before supersonic vehicles could be designed free of panel flutter. The experimental and theoretical research generated by flight experience with panel flutter is evidenced by the many recent papers on the subject.

LANDING LOADS

The first four landings of the X-15 pointed out certain deficiencies in the design of the original gear system, caused primarily by insufficient energy absorption of the shock struts. The main-gear system was modified simply by replacing the shock strut with struts having greater energy-absorbing characteristics and by strengthening the backup structure. The solution to the nose-gear problem was accomplished by using a floating piston inside the strut to separate the gas and oil and thus prevent foaming due to rapid gear extension. Although all subsequent landings of the X-15 have been accomplished without incident, the landing dynamics of the airplane are somewhat unusual.

The airplane has been instrumented to measure gear loads, gear travel, and accelerations. Figure 2 shows the main-gear shock-strut force and travel measured on a typical X-15 landing. The upper curve is the strut travel, and the lower curve is the strut force measured from time after main-gear touchdown. The sketches at the top of the figure identify the landing sequence. Note that both the shock-strut force and travel are appreciably higher during the second reaction on the main gear, following the nose-gear touchdown, than for the initial portions of the landing. These high values are due to several factors, but primarily to the main-gear location well back of the airplane's center of gravity, the pronounced aerodynamic down loads on the tail, the negative wing lift

during this portion of the landing, and the airplane inertial loads. Since the maximum shock-strut force occurs during the second reaction, the usual parameters such as airplane sinking speed, angle of attack, and forward speed at touchdown cannot be used to define adequately the design conditions of the X-15 type of landing gear. For convenience, the time histories of only one gear are shown, since all of the landings have been nearly symmetrical.

AERODYNAMIC AND STRUCTURAL HEATING

Aerodynamic and structural heating are major factors affecting hypersonic and reentry vehicles. During the X-15 program, a considerable amount of heating data, in the form of measured temperatures, has been obtained. These data, together with simplified calculations, have been used to define the safe operating environment and, for certain flight conditions, to obtain heat-transfer coefficients.

Surface Temperatures

The type of X-15 flight of interest from the standpoint of reentry heating is illustrated in Fig. 3. The upper plot shows the time variations of altitude and velocity, and the lower plot shows the variation of airplane angle of attack with time. Also shown is the temperature of a representative point on the lower surface of the wing. As can be seen, the velocity, altitude, and angle of attack change rapidly and, for this reason, a flight of this type is not the most desirable for obtaining heat-transfer-coefficient data. However, heat transfer during the reentry type of flight can sometimes be inferred from comparisons of calculated and measured skin temperatures, as illustrated in Fig. 4. These results are for the wing skin on the lower surface well back of the stagnation region. The data show that this point on the wing appears to experience some laminar flow, as indicated by the dashed curve. Calculations based on all turbulent heat transfer

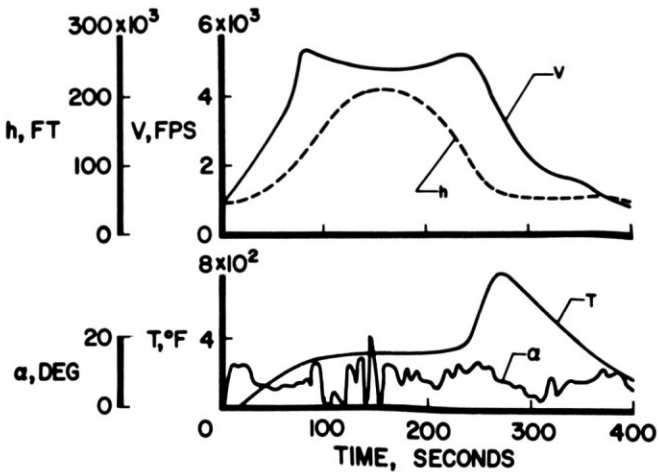

Fig. 3. Typical high-altitude flight.

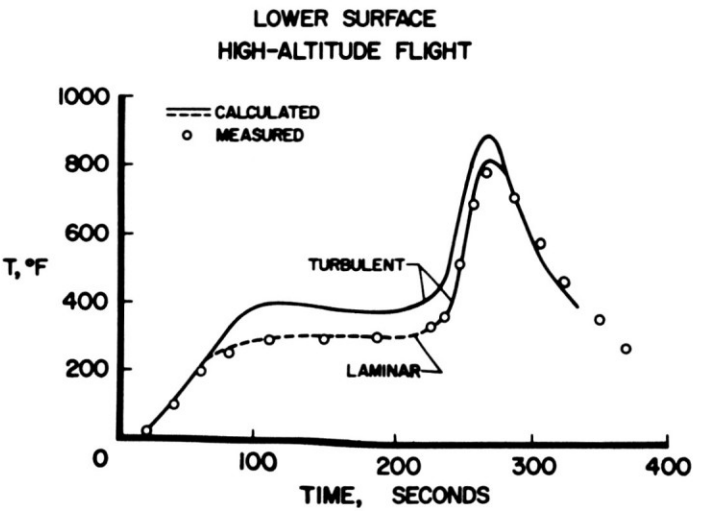

Fig. 4. Wing skin temperatures.

give higher temperatures than were measured during the exit phase of the flight, greater cooling during the ballistic portion, and higher values of maximum temperature during reentry. Calculations based on laminar flow during the latter part of the exit phase and the ballistic phase result in more satisfactory agreement between calculated and measured values. The exact cause of the transition from turbulent to laminar and back to turbulent is not known; however, the results in Fig. 4 show that, if the boundary layer is known to be either laminar or turbulent, the skin temperatures can be calculated with reasonable accuracy.

Internal Temperature

The variations of temperature through the wing structure for the high-altitude flight of Fig. 3 are shown in Fig. 5, in which the temperature histories for the front spar of the wing at the midsemispan are presented. The sketch illustrates the thermocouple location on the lower skin, the lower spar cap, the web, and the upper skin. The numeral adjacent to each thermocouple identifies the corresponding curve. The time of 275 sec corresponds to the time of maximum temperature difference of 700°F between the lower skin and the spar web. From the standpoint of thermal stresses in the structure, the temperature gradient together with the temperature level defines the most severe condition on each flight. The measured data give the temperature levels, but with the limited number of thermocouples on the spar, the complete thermal gradient cannot be obtained from the flight measurements and must, therefore, be obtained from analysis.

Calculated gradients are compared with flight data for the time of maximum gradient in Fig. 6. The temperature is shown as a function of the wing thickness measured from the lower surface. The solid curve was obtained from calculations,

and the data points are from the flight measurements made at the locations shown in the sketch. For these calculations, the heat transfer to the external skin was determined, first, on the basis of the time history presented in Fig. 5. This heat input was used to compute thermal gradients in the spar, including part of the cover sheet. Figure 6 shows the good agreement between calculated and measured temperatures at the four thermocouple locations in the sketch.

The maximum temperatures measured at various locations on the X-15 during the flight program are summarized in Fig. 7. These temperatures did not

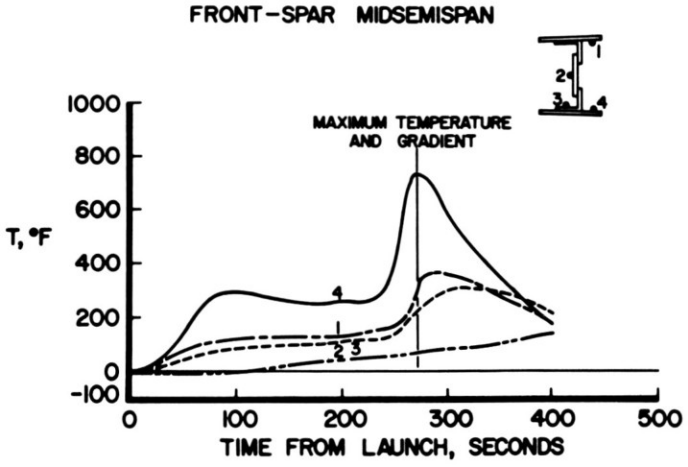

Fig. 5. Wing-spar temperatures during high-altitude flight.

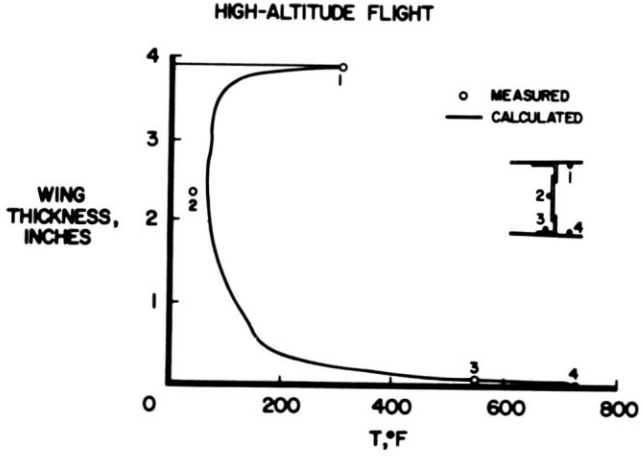

Fig. 6. Calculated spar temperatures at time = 275 sec.

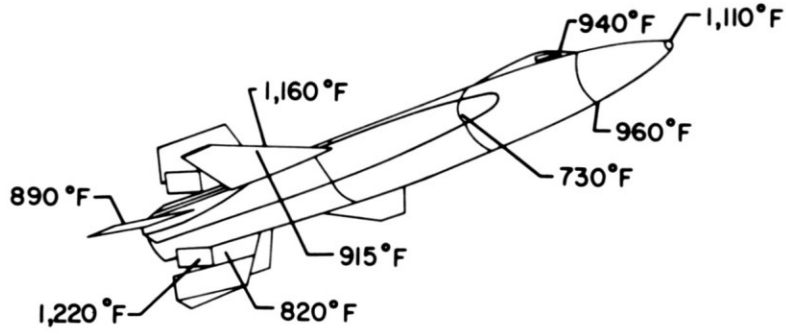

Fig. 7. Summary of maximum temperatures.

all occur on the same flight; however, they serve to illustrate the highest temperature levels that the structure has experienced, with the exception of local hot spots which are discussed subsequently.

STRUCTURAL PROBLEMS

Structural problems have developed on the X-15 fuselage and wing as a result of heating or thermal stress.

Skin Buckling

The first temperature problem occurred on the side-fairing panels along the liquid-oxygen tank before the X-15 was flown. Pronounced elastic buckles appeared in the panels as a result of tank contraction when the tanks were filled for the first time. Buckling was relieved by adding an expansion joint to the tunnel fairing near the wing leading edge.

After the first flight above a Mach number of 4, several permanent buckles were formed in the outer sheet of the fairing panels. Since these fairing panels are required to carry local airloads only, the buckles did not seriously affect the structural integrity. The maximum temperatures measured on these panels during the flight in which buckling occurred are shown in Fig. 8 for two fuselage stations in the area of the liquid-oxygen tank. The insert is a photograph of a typical buckle in the fairing panel. This buckle occurred near the wing leading edge. The scales, graduated in inches, show the extent of the buckle. Depth of the buckle is about ¼ in. No temperature measurements were made on the liquid-oxygen tank. The temperatures shown occurred after engine shutdown, which, on this flight, left about 20 percent of the fuel still in the tanks. The cold tank, about −260°F for liquid oxygen, together with the high skin temperatures on the fairing resulted in large gradients and, hence, the buckle. The significant result was that the thermal gradients between the liquid-oxygen tank and the

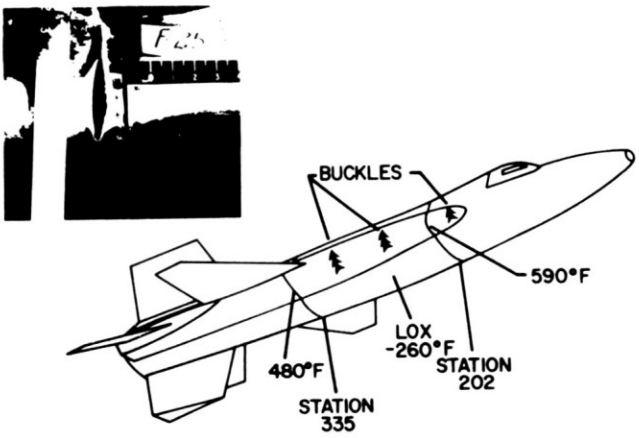

Fig. 8. Maximum side-fairing temperatures during flight to $M_{max} = 4.43$.

fairings were actually higher than calculated for the original design, which shows that even minor deviations from the design environment can seriously affect local structural areas. The design was based on complete fuel burnout before the maximum skin temperatures were encountered. As a result of this experience, additional expansion joints were installed in the fairing to increase expansion capacity. To date, this modification has prevented additional permanent buckles for similar flights at higher temperatures.

Glass Failure

The choice of tempered glass for the windshield of the X-15 was based on data which indicated that outer-surface temperatures near 1000°F could be expected, with a differential temperature between surfaces of 750°F. Although the selected glass withstood thermal tests to temperatures and gradients about 1½ times the expected flight values, one of the windshield panels fractured during a flight to maximum speed. The glass fragments remained in place during the remainder of the flight. A photograph of the fractured glass is shown in Fig. 9. The fracture pattern is typical of tempered glass. Examination of the pattern showed that failure started near the center of the upper edge of the windshield. The cause of the failure was traced to a thermal buckle of the retainer frame which created a local hot spot in the glass at this point due to stagnation-point heating. After this failure, the retainer was increased in thickness, and the material was changed to one with a lower coefficient of expansion in order to prevent thermal buckling and, hence, the local hot spots.

Damage to Wing Leading Edge

Structural problems have developed on the wing leading edge of the X-15 because of thermal gradients and local hot spots not detected by thermocouples.

In order to study the overall temperature levels on the wing structure, temperature-sensitive paints are being used. These paints change color at known temperature levels and retain the color after cooling. The paint is applied to the surface of the wing and tail before flight, and the color changes and patterns are examined after the flight to determine gross skin temperatures.

Figure 10 is a photograph showing the postflight paint patterns on the upper surface of the wing. The dark areas are regions of temperatures over 600°F,

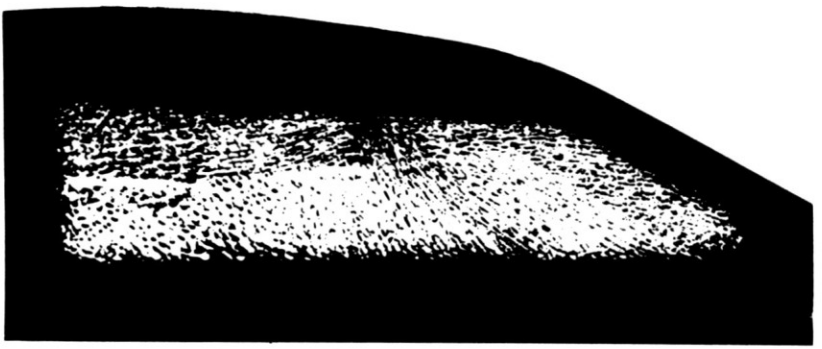

Fig. 9. Damaged windshield glass following flight to $M_{max} = 6.04$.

Fig. 10. Temperature-sensitive-paint patterns.

and the lighter areas are regions of temperatures less than 400°F. The heat sink of the internal structure is evident. Although not clearly seen in this photograph, areas of high temperatures begin at four points on the wing leading edge and extend back over the wing. These areas start at the expansion joints in the leading-edge heat sink. On the first flight above Mach 5, the areas of local heating were much more pronounced. The temperature distribution in the vicinity of these slots on this flight is shown in Fig. 11. These data were obtained from paint patterns, since no thermocouples were located in this region; however, the paint colors obtained were correlated with thermocouple data at other points on the wing. This figure shows a segment of the wing leading edge, the expansion joint, and a section of the lower skin. The expansion joints are slots, about 0.08 in. wide, cut in the heat sink. The average leading-edge temperature was 830°F, and just outboard of the slot on the leading edge is a small area with temperatures above 1000°F. An area between 970°F and 1000°F extends rearward on the skin about 8 in., and the average skin temperature away from the slot is below 800°F.

On this flight, permanent interrivet buckles were formed directly behind the three outboard slots of the leading edge. The type of buckle and the location are illustrated by the upper sketch in Fig. 12. This sketch shows a portion of a leading-edge heat sink, the expansion slot, the external skin with the buckle, and the fastener location. Note that the fastener spacing directly behind the slot is wider than the spacing along the solid portion of the leading edge. Subsequent analysis of the leading-edge structure indicated that several factors contributed to the permanent buckling of the skin. One factor is the thermal stress in the skin caused by high gradients around the local hot spots. Another factor is the wide fastener spacing through the leading edge at the expansion slot. A third reason for the buckle is that the original segmentation of the leading-edge heat sink did not adequately relieve the thermally induced compressive

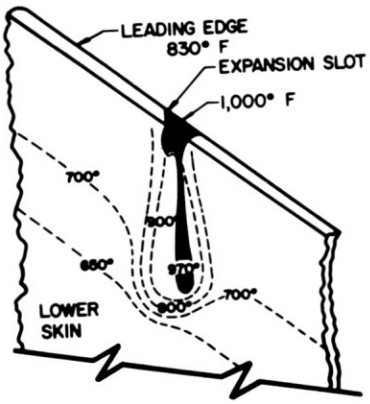

Fig. 11. Temperature distribution aft of leading edge expansion slot.

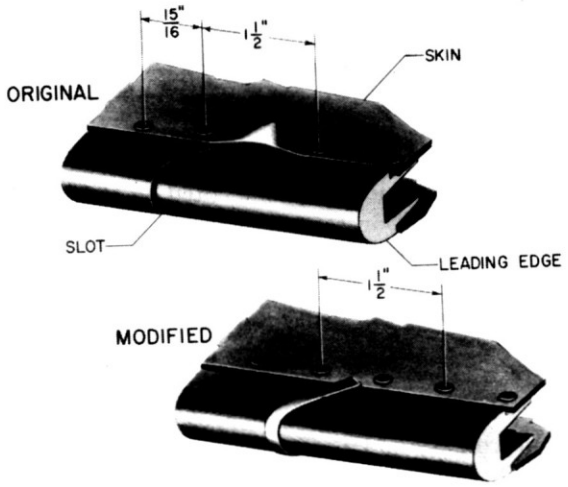

Fig. 12. Wing skin buckle following flight to $M_{max} = 5.28$.

loads. The skin at the slot acted as a splice plate for the heat-sink bar and thus was buckled in compression.

In order to minimize this buckling problem, three design changes have been made. Two of the changes are shown on the lower sketch of Fig. 12. An 0.008-in. thick Inconel tab welded over one edge was installed over each slot to prevent tripping the boundary layer and thus to minimize the local hot spot. A fastener was added at the slot to decrease the fastener spacing and to increase the skin buckling allowable. In order to reduce the loads that the skin splice must carry at each slot, the third change was to add an expansion slot with a shear tie and cover tab in three of the outboard segments of the leading edge. Since these changes were made, no damage has occurred in the leading edge.

FLIGHT CONTROL SYSTEMS

Handling Qualities

The structural heating and maximum temperatures experienced during a high-altitude recovery depend to a large extent on the ability of the pilot to fly the proper trajectory. In turn, this ability is entirely dependent on the aircraft's stability at the angles of attack and velocities experienced during reentry.

The X-15 handling qualities have been assessed from pilot opinion and from data obtained during flight. The launch from the modified B-52 airplane and the initial climbout are common to all flights. Immediately after launch the engine is started and the X-15 rotated to the desired climb attitude. The aerodynamic qualities at an altitude of 45,000 ft and subsonic speed are considered to be excellent. Mild buffet at subsonic speed has been encountered above a 10°

angle of attack, but buffet is absent above Mach 1. A nosedown trim change which occurs at low supersonic speed is only slightly objectionable to the pilot.

During the exit phase the airplane is very stable, and damping appears to be adequate even without artificial damping. The longitudinal acceleration produced by the engine thrust has not impaired the pilot's ability to fly the airplane. At engine shutdown, there have been no transient motions or evidence of thrust misalinement. As the airplane passes through an altitude of 145,000 ft, a decay in the response to aerodynamic controls is noted by the pilot, and reaction controls are required. The reaction controls have proved to be very effective; the response in roll and yaw is good, and pitch response on one flight was more than desired. This experience indicates that an augmentation system for the reaction controls would improve controllability during the ballistic portion of the flight.

The reentry is flown at relatively high angles of attack and under rapidly changing conditions of dynamic pressure and velocity, with associated changes in aircraft stability and response. At angles of attack above 8°, the pilot has great difficulty controlling the lateral and directional motions to prevent divergence without stability augmentation. Hence the stability augmentation system on the X-15, which provides rate damping about all three axes, has a significant effect on pilot opinion.

The approach and landing, which caused much concern during the initial phase of the X-15 flight program, has been reduced to a routine operation as a result of experience. The pilot has considerable flexibility in maneuvering to a designated landing point. Handling qualities and airplane response are considered to be excellent, although vertical velocity averages 250 fps prior to the landing flare. The landing flare is initiated from the pilot's estimate of the height necessary to reduce the sink rate and arrive level close to the ground. During the ground runout, the X-15 has good inherent directional stability, but is not provided with directional control.

STABILITY AUGMENTATION SYSTEM (SAS)

The X-15 stability and control characteristics at high angles of attack are summarized in Fig. 13, in which angle of attack is shown as a function of velocity. The solid line is the maximum trim limit, and the dashed line is the subsonic buffet boundary. The light area represents the range of angle of attack and velocity in which the basic airplane is controllable without augmentation, and the shaded area represents the region where the X-15 is controllable with the stability augmentation system in operation. The hatched area represents regions of instability with or without the stability augmentation system. In order to perform reentries within the design limit of dynamic pressure and, hence, heating rates, it is necessary to fly at high angles of attack at high velocities. From this figure it can be seen that stability augmentation is essential.

The augmentation system in use on the X-15 is a simple three-axis damper system, as illustrated by the functional diagram of Fig. 14. The essential components of the pitch, roll, and yaw channels of the system are the indicated gyros, cockpit gain selectors, electronics, and servos. The outputs of the servos go to their respective control surfaces. The unique features of the system are

cockpit gain selection and the interconnection required for operation of the right-hand and left-hand horizontal stabilizers which provide both pitch- and roll-damper input. Also shown is a yaw-rate input to the roll axis. This interconnection is necessary for stability at high angles of attack, primarily because of the roll input of the lower rudder. The gain-selector settings of 8-6-8 indicated

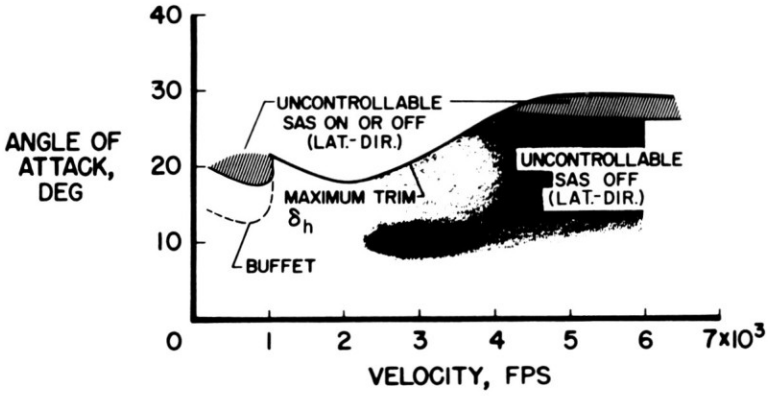

Fig. 13. Summary of predicted stability and control.

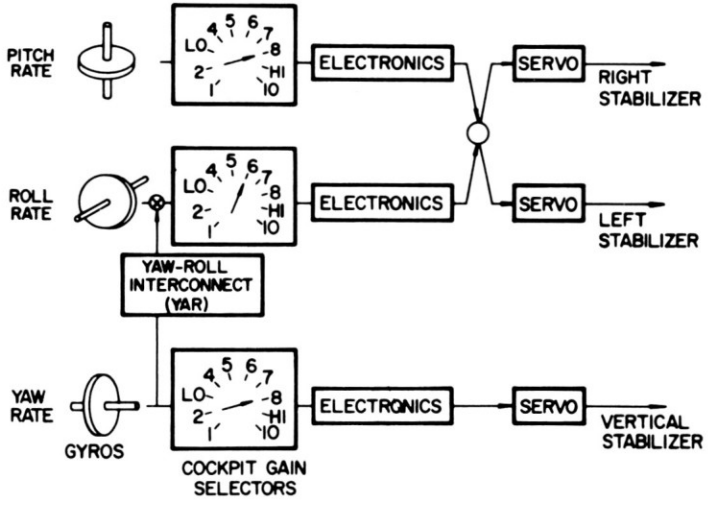

Fig. 14. Functional diagram of SAS.

for pitch, roll, and yaw, respectively, are the normal settings. Although experience with this system has shown it to be reliable, several interesting problems have developed during use.

Early in the X-15 program, unwanted limit cycles or continuous oscillation sustained by the stability augmentation system were observed. The limit cycles were caused by hysteresis and rate limiting which produced considerable phase lag. The frequency of this limit cycle was about 3.2 cps, and the airplane amplitude of motion was about 1° total change in bank angle. As a means of reducing the limit cycle to acceptable amplitudes, the SAS electronic filter was modified. The reduced lag of the modified filter greatly reduced the amplitudes of the limit cycle so that the problem was essentially eliminated. Later in the program, it became apparent during ground tests that it was possible to excite and sustain a system-airplane vibration at 13 cps with the modified filter. However, initial flights with this filter failed to produce the vibration. Several flights later, during recovery from a high-altitude mission, the pilot reported a severe vibration. This vibration was triggered by pilot inputs at low dynamic pressure and continued until the SAS gain was reduced slightly and dynamic pressures increased to about 1,000 lb per sq ft. Fortunately, the amplitude of the shaking was limited by the rate limiting of the control-surface actuators. Figure 15 illustrates the mechanics of this phenomenon. The lightly damped horizontal-stabilizer surfaces, represented by the flexible beams with masses, were excited at their natural frequency of 13 cps by the pilot inputs to the control system. The inertial reaction of the fuselage to this vibration was picked up by the gyros so that the SAS was able to sustain the vibration with inputs to the control surfaces.

Because of the closed-loop nature of the problem, restrictions in allowable gain exist at the structural frequencies, as shown in Fig. 16. The hatched areas represent unstable regions. If the curves intersect these boundaries, which represent restrictions in gains at the structural frequencies of the horizontal tail at 13 cps and 30 cps, a sufficient condition exists for a sustained oscillation.

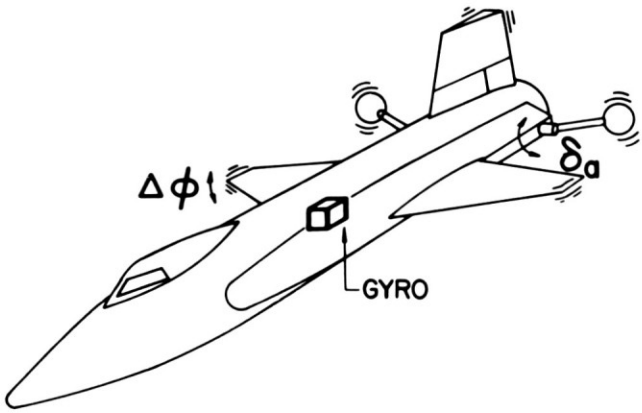

Fig. 15. Mechanism of vibration.

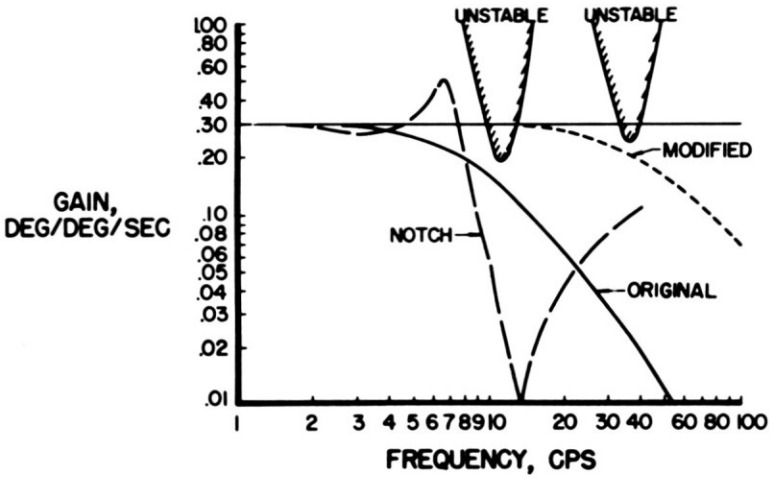

Fig. 16. Effect of filters on high-frequency stability.

The modified filter used during the previously discussed altitude flight intersects the first boundary. A vibration, therefore, would be expected at 13 cps. The original filter is seen to be free of the 13-cps vibration, but produces unacceptable limit-cycle characteristics at the critical flight conditions. One way of avoiding both problems is to use a notch filter. This filter was designed to give a minimum phase lag at limit-cycle frequencies. The notch filter has been thoroughly checked out by ground tests, but not in flight.

In general, the X-15 airplane with the stability augmentation system has sufficient damping over the entire aerodynamic region. In the ballistic region, aerodynamic controls become ineffective and the use of reaction controls is required. The X-15 has been successfully flown through the ballistic region with the reaction controls and has been properly positioned for the reentry maneuver. However, experience in flight indicates that an augmentation system for the reaction controls would greatly improve the control characteristics of the airplane and provide a good backup damping system for the stability augmentation system during the setup for the reentry portion of the high-altitude flights.

Adaptive Control System

A flight program to investigate advanced flight control systems is in progress with the X-15. At present, a system based on the self-adaptive principle is installed in one of the aircraft. This system, as the name implies, automatically adapts itself in order to provide essentially constant damping and aircraft frequency in combination with the control system as a vehicle encounters flight conditions of varying aerodynamic control-surface effectiveness. The principle of operation of this system is illustrated in Fig. 17. Pilot inputs to the surface actuators are applied by mechanical links. At the same time, electrical inputs,

proportional to stick displacement, are supplied to both the pitch and roll channels. The electrical input to each axis is shaped by a simple network which has the dynamic response that is desired of the aircraft in that axis. Sufficient lead is added and gains increased enough so that the remainder of the loop will have a transfer function which approaches unity. When this condition is reached, the response of the aircraft will be that of the model. The gain changer operates by monitoring the limit-cycle amplitude and adjusting the gain to maintain a constant amplitude. In addition to the components shown, the system requires inputs proportional to angle of attack and airplane attitude. Basic damping augmentation is provided by attitude-rate feedback in all three axes.

The self-adaptive control system provides automatic blending of the aerodynamic and reaction controls, which makes it possible for the system to operate the vehicle throughout the complete mission. The principle of this technique is illustrated in Fig. 18. When the system gains on all three axes reach 80 percent of maximum, the reaction-control channels are activated. The solenoid valves which are actuated by electrical commands from the pilot will not, however, operate until needed. A dead spot in the system allows aerodynamic controls to be used to the fullest extent to maintain constant response until the pure ballistic condition is approached. In this condition, the thrust limitations of the reaction jets cause a slower response. Even here, the rate feedback will provide rate damping and rate-command operation. On entry, the aerodynamic controls become effective and, as the system gains fall below 60 percent of maximum, the reaction-control channel is deactivated. The 60 percent value was selected because studies showed that occasional servo activity in the ballistic regime could lower the gain, and thereby deactivate the reaction controls.

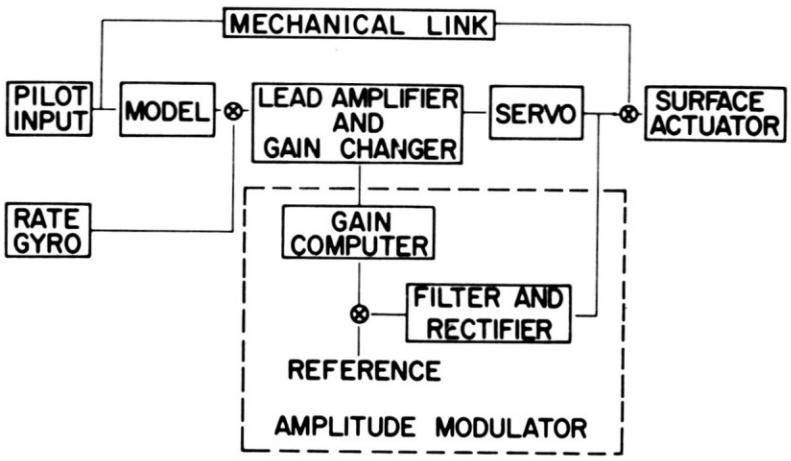

Fig. 17. Adaptive concept.

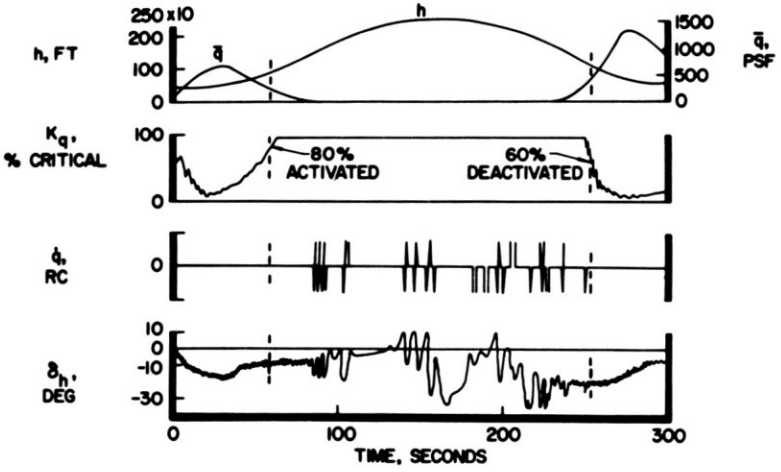

Fig. 18. Controls blending.

Four successful demonstration flights of the self-adaptive system have been made to check system operation. This flight program will be continued to evaluate the adaptive principle, and to provide research information for comparison with other types of control systems.

CONCLUDING REMARKS

The X-15 flight program has been conducted without undue problems with the flight systems and without encountering extreme structural temperatures. Comparison of calculated and measured internal temperatures has shown that satisfactory thermal gradients for the X-15 structure can be calculated from heat-transfer data inferred from measured skin temperatures.

In general, the simple three-axis damper system for stability augmentation and the hot-structure concept used on the X-15 airplane have proved to be satisfactory. Although the airplane has adequate stability and control to insure flight within the design capabilities, structural problems have developed as a result of local hot spots and discontinuities in the structural elements.

Although many of the problems encountered in this program pertain to the X-15 only, similar problems may be expected on all hypersonic and reentry vehicles until additional research provides adequate design information in these problem areas.

SYMBOLS

F_t = horizontal-tail aerodynamic load
h = altitude
K_q = pitch-rate gain

L = lifting force
M_{max} = maximum Mach number
$\bar{q}$ = dynamic pressure
$\bar{q}_{RC}$ = pitch acceleration due to reaction controls
T = temperature
V = velocity
V_{v_o} = airplane sinking speed at initial touchdown
W = airplane landing weight
α = airplane angle of attack
α_0 = initial airplane angle of attack at touchdown
Δ_φ = peak-to-peak amplitude of limit cycle in roll
δ_a = total aileron deflection
δ_h = horizontal-tail angle

BIBLIOGRAPHY

Finch, Thomas W., and Gene J. Matranga, "Launch, Low-Speed, and Landing Characteristics Determined from the First Flight of the North American X-15 Research Airplane," *NASA TM X-195*, 1959.

McKay, James M., "Measurements Obtained During the First Landing of the North American X-15 Research Airplane," *NASA TM X-207*, 1959.

Flight Research Center, "Aerodynamic and Landing Measurements Obtained During the First Powered Flight of the North American X-15 Research Airplane," *NASA TM X-269*, 1960.

Walker, Harold J., and Chester H. Wolowicz, "Theoretical Stability Derivatives for the X-15 Research Airplane at Supersonic and Hypersonic Speeds Including a Comparison with Wind-Tunnel Results," *NASA TM X-287*, 1960.

Stillwell, Wendell, H., and Terry J. Larson, "Measurement of the Maximum Speed Attained by the X-15 Airplane Powered with Interim Rocket Engines," *NASA TN D-615*, 1960.

Stillwell, Wendell, H., and Terry J. Larson, "Measurement of the Maximum Altitude Attained by the X-15 Airplane Powered with Interim Rocket Engines," *NASA TN D-623*, 1960.

Saltzman, Edwin J., "Preliminary Full-Scale Power-Off Drag of the X-15 Airplane for Mach Numbers from 0.7 to 3.1," *NASA TM X-430*, 1960.

Reed, Robert D., and Joe D. Watts, "Skin and Structural Temperatures Measured on the X-15 Airplane During a Flight to a Mach Number of 3.3," *NASA TM X-468*, 1961.

Matranga, Gene J., "Launch Characteristics of the X-15 Research Airplane as Determined in Flight," *NASA TN D-723*, 1961.

Holleman, Euclid C., and Donald Reisert, "Controllability of the X-15 Research Airplane with Interim Engines During High-Altitude Flights," *NASA TM X-514*, 1961.

McKay, James M., and Betty J. Scott, "Landing-Gear Behavior During Touchdown and Runout for 17 Landings of the X-15 Research Airplane," *NASA TM X-518*, 1961.

Matranga, Gene J., "Analysis of X-15 Landing Approach and Flare Characteristics Determined from the First 30 Flights," *NASA TN D-1057*, 1961.

Saltzman, Edwin J., "Preliminary Base Pressures Obtained From the X-15 Airplane at Mach Numbers from 1.1 to 3.2," *NASA TN D-1056*, 1961.

Taylor, Lawrence W., Jr., "Analysis of a Pilot-Airplane Lateral Instability Experienced with the X-15 Airplane," *NASA TN D-1059*, 1961.

Yancey, Roxanah B., Herman A. Rediess, and Glenn H. Robinson, "Aerodynamic-Derivative Characteristics of the X-15 Research Airplane as Determined from Flight Tests for Mach Numbers from 0.6 to 3.4," *NASA TN D-1060*, 1962.

Kordes, Eldon E., and Richard B. Noll, "Flight Flutter Results for Flat Rectangular Panels," *NASA TN D-1058*, 1962.

Taylor, Lawrence W., Jr., and George B. Merrick, "X-15 Airplane Stability Augmentation System," *NASA TN D-1157*, 1962.

Jordan, Gareth H., Norman J. McLeod, and Lawrence D. Guy, "Structural Dynamic Experiences of the X-15 Airplane," *NASA TN D-1158*, 1962.

Hoey, Robert G., and Richard E. Day, "Mission Planning and Operational Procedures for the X-15 Airplane," *NASA TN D-1159*, 1962.

Banner, Richard D., Albert E. Kuhl, and Robert D. Quinn, "Preliminary Results of Aerodynamic Heating Studies on the X-15 Airplane," *NASA TM X-638*, 1962.

McKay, James M., and Eldon E. Kordes, "Landing Loads and Dynamics of the X-15 Airplane," *NASA TM X-639*, 1962.

Kordes, Eldon E., Robert D. Reed, and Alpha L. Dawdy, "Structural Heating Experiences on the X-15 Airplane," *NASA TM X-711*, 1962.

Keener, Earl R., and Chris Pembo, "Aerodynamic Forces on Components of the X-15 Airplane," *NASA TM X-712*, 1962.

Hopkins, Edward J., David E. Fetterman, Jr., and Edwin J. Saltzman, "Comparison of Full-Scale Lift and Drag Characteristics of the X-15 Airplane with Wind-Tunnel Results and Theory," *NASA TM X-713*, 1962.

Walker, Harold J., and Chester H. Wolowicz, "Stability and Control Derivative Characteristics of the X-15 Airplane," *NASA TM X-714*, 1962.

White, Robert M., Glenn H. Robinson, and Gene J. Matranga, "Résumé of Handling Qualities of the X-15 Airplane," *NASA TM X-715*, 1962.

Petersen, Forrest S., Herman A. Rediess, and Joseph Weil, "Lateral-Directional Control Characteristics of the X-15 Airplane," *NASA TM X-726*, 1962.